A Generalized Physics-Based Circuit Model for Predicting Nonlinear Properties of Magnetic Materials.

Project Leads: Leon M. Tolbert (UTK), Gong Gu (UTK), Daniel Costinett (UTK)

Graduate Students and Research Faculty/Associates: Sadia Binte Sohid (UTK), Noah Wilding (UTK), Christian Harmon (UTK)

Project Duration: 8/2022 – 07/2026

Funding Source: Office of Naval Research (ONR)

Summary

The nonlinear and frequency-dependent behavior of magnetic materials continues to limit the accuracy of conventional magnetic models, especially in high-frequency power electronics where core loss and permeability vary with excitation conditions. To overcome the limitations of conventional models, the spherical form of the LLG equation (sLLG): $\begin{bmatrix}\frac{d\theta}{dt}\\ \frac{d\varphi}{dt}\end{bmatrix} = \mu_0\frac{\gamma}{(1+\alpha^2)}\begin{pmatrix}\alpha & 1\\ -\frac{1}{sin\theta} & \frac{\alpha}{sin\theta}\end{pmatrix}\begin{bmatrix}H_{eff}^{\theta}\\ H_{eff}^{\varphi}\end{bmatrix}$ is used to model magnetization dynamics. An important advantage of the sLLG is that it inherently preserves the constant magnetization magnitude, avoiding the additional numerical constraints required in the Cartesian LLG model. The spherical LLG approach reproduces the same overall hysteresis behavior as the full LLG formulation while greatly reducing simulation time.

Effects due to magnetic anisotropy as well as domain coupling are incorporated into the dynamics governing the system. Domain magnetic moments change over time when subjected to an external magnetic field, as illustrated in Fig. 2. Magnetic anisotropy is illustrated in Fig. 3 and shows how anisotropic materials prefer to align their magnetic moments with the easy axis. To extend the model beyond a single-domain approximation, the material is represented as a coupled two domain system in which neighboring domains interact through domain-wall energy, as illustrated in Fig. 4.

To reduce the total computation power and time required of this model, the precessional motion term can be omitted as it has a negligible effect on energy loss through damping. The resulting simplified spherical LLG (ssLLG) $\frac{d\theta}{dt} = \mu_0\frac{\gamma}{(1+\alpha^2)}\left(\alpha H_{eff}^{\theta} + H_{eff}^{\varphi}\right)$ equation preserves dominant system dynamics while requiring far less simulation time than the cartesian LLG approach as illustrated in Fig. 5.

The coupled model accounting for both anisotropy and domain wall motion was simulated, and results comparing the sLLG and ssLLG are shown in Fig. 6. The ssLLG model shows good alignment with the full sLLG model while requiring minimal runtime.

Future project work includes incorporation of multiple coupled domains as well as temperature dependence of material properties such as anisotropy constant, magnetic saturation, and exchange stiffness. Collaboration with magnetics material developers at the University of Pittsburgh, Northeastern University and Dartmouth University will aid in ensuring the model can predict the behavior of new magnetic materials.

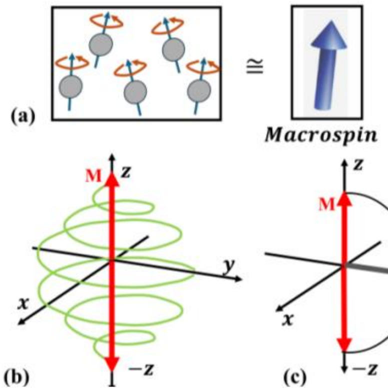

Fig. 1. (a) Equivalent macrospin model representing the collective magnetization (M) of the system under an effective magnetic field (H_{eff}) (b) Dynamic motion of a dipole moment governed by the LLG equation. (c) Two equilibrium magnetization states predicted by energy minimization theory.)

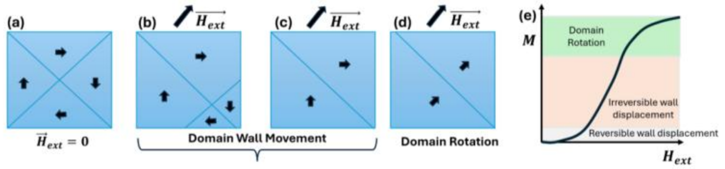

Fig. 2. Illustration of the progression of magnetization in a crystal under an applied magnetic field. Starting from the demagnetized state in (a), where domains with different magnetization orientations are present, the application of an external field initiates domain wall motion, as shown in (b) and (c). This wall movement leads to the growth of domains aligned with the field direction. As the field strength increases further, the process transitions from domain wall motion to rotation of magnetization, as shown in (d). The corresponding magnetization curve in (e) highlights the distinct regions associated with reversible wall motion, irreversible domain wall displacement, and domain rotation

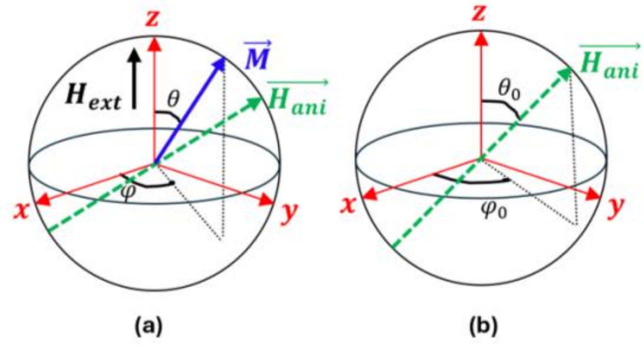

Fig. 3. Illustration of the magnetization vector M and anisotropy field H_{ani} in spherical coordinates, defined by angular components (θ,φ), and (θ_0 ,φ_0), respectively.

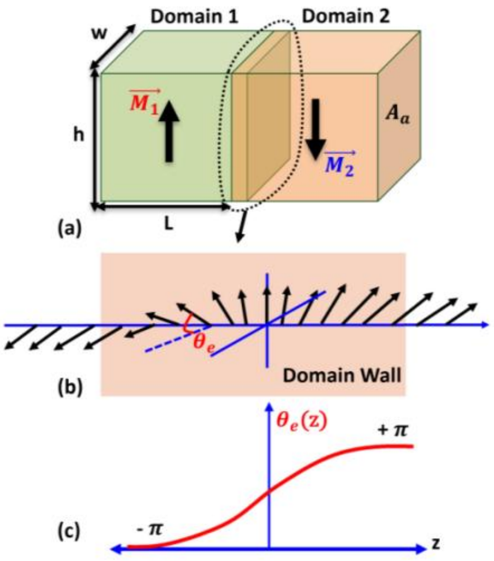

Fig. 4. Two-domain model: (top) domains 1 and 2 magnetized 180° apart; (middle) spins rotate through angle θe in the wall, balancing exchange and anisotropy torques; (bottom) continuous θe (z) profile across the domain wall.

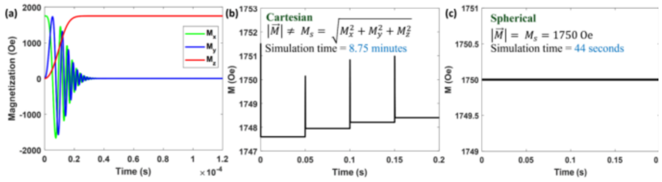

Fig. 5. Comparison of LLG simulations in cartesian and spherical coordinates. (a) Magnetization dynamics computed using both cartesian and spherical coordinates. (b) The cartesian model shows deviation from the constant magnitude condition ($|M| = Ms$) and requires a longer runtime (8.75 min). (c) The spherical model maintains constant $|M| = Ms$ with faster runtime (44 s).

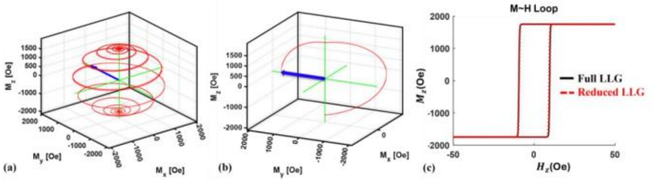

Fig. 6. Here, Ms = 1750 Oe, α = 0.1, f = 10 kHz [11]. Dynamic motion using (a) the full LLG equation and (b) the reduced LLG equation. The aligned M−H loops for both cases confirm consistency in magnetization behavior

Co-located SMRs, hyperscale data centers, and energy storage for increased system resiliency

Project Lead: Leon M. Tolbert (UTK) **Graduate Students and Research Faculty/Associates:** Mariana Espinola (UTK), Mateus Silva (UTK), Hari Naicker (Nuclear Engineering, UTK), Justin Zondor (NE, UTK), Carlos G. Zevallos, Shiyuan Fan (UTK), Jamie Coble (Nuclear Engineering, UTK)
Project Duration: July 2025 – June 2026
Funding Source: UT-ORII

Summary

This project proposes a grid-connected microgrid architecture centered on a Small Modular Reactor (SMR) as the primary power source for a hyperscale data center. The proposed system considers the integration of thermal energy storage (TES), a Battery Energy Storage System (BESS), and a coordinating Energy Management System (EMS) to support the facility's load while enabling potential participation in electricity markets through ancillary service provision.

The data center load is being represented using simplified demand scenarios intended to approximate the scale and variability expected in next-generation hyperscale deployments. These scenarios are designed to capture characteristics associated with both inference and training workloads, which can exhibit large magnitude and rapid temporal variation.

In the proposed operating strategy, the SMR is assumed to operate near full capacity to maintain a high capacity factor, while the BESS is used to compensate for short-term mismatches between quasi-steady nuclear generation and fluctuating IT load. The electrical storage subsystem is currently represented using a containerized lithium-ion BESS architecture with an initial target rating of approximately 120 MW / 480 MWh for transient smoothing and contingency support; however, storage sizing remains under evaluation as part of the ongoing system design process. Waste heat recovered from the SMR is also considered as a potential resource for thermal energy storage and cogeneration applications that may improve site-level energy utilization and Power Usage Effectiveness (PUE).

A hierarchical EMS framework is being developed to coordinate dispatch across SMR, BESS, and TES subsystems. At the supervisory level, the controller is intended to maintain reliable power delivery to the data center while respecting SMR ramp-rate constraints and managing storage utilization. Local control layers regulate battery power response, TES scheduling strategies, and grid import/export behavior under representative operating conditions.

Current work focuses on system architecture definition, component sizing assumptions, and the development of coordinated control strategies under representative load scenarios and grid operating conditions. The modeling framework is intended to support future evaluation of techno-economic performance, regulatory and interconnection considerations, and scalability to multi-module SMR configurations for large data center campuses.

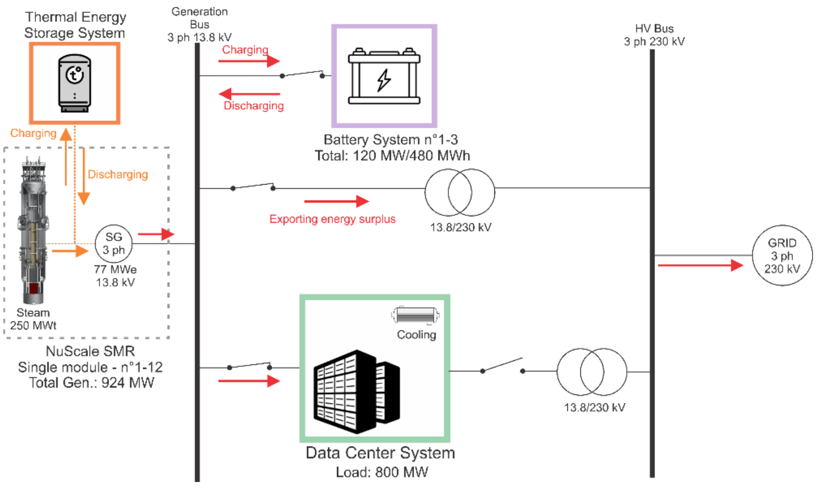

Figure 1. Integrated SMR–TES–BESS architecture supplying a hyperscale data center with grid interconnection capability.

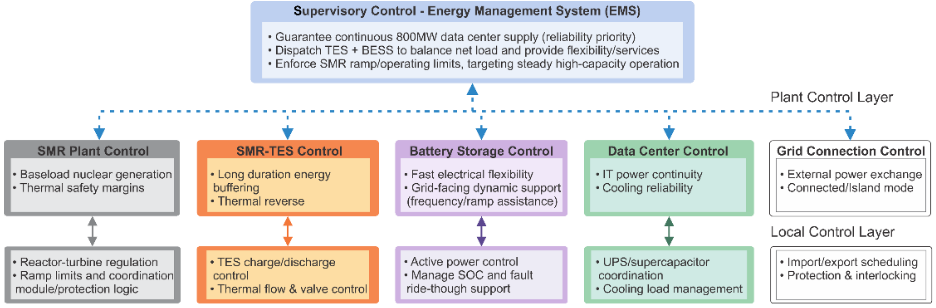

Figure 2. Hierarchical supervisory and local EMS control structure coordinating SMR operation, storage dispatch, and data center load support.

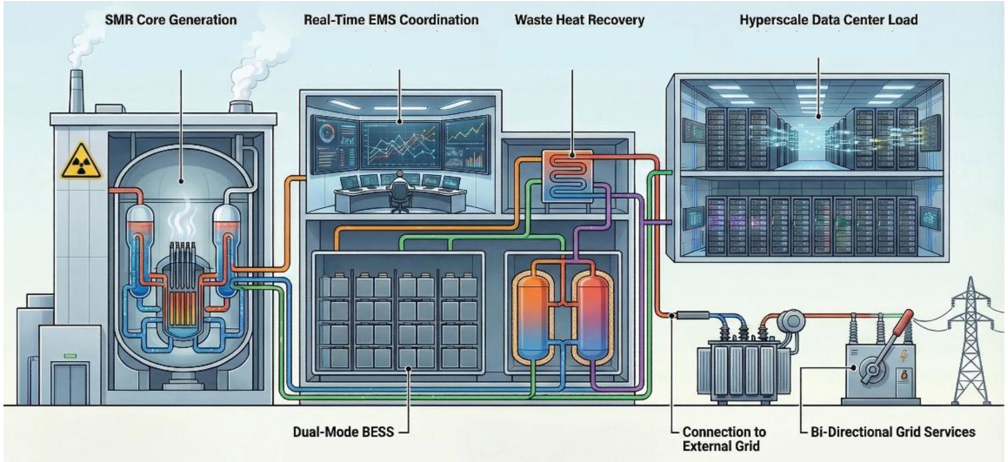

Figure 3. Representative operating scenarios for coordinated SMR–TES–BESS support of hyperscale data center operation.